

# Modeling of Multiple Scattering from an Ensemble of Spheres in a Laser Beam

Vladimir I. Ovod\*

(Received: 12 October 1998; resubmitted: 12 February 1999)

## Abstract

This paper details the results of upgrading an effective numerical technique (derived for multiple-scattering simulations in photon correlation/cross-correlation with a plane-wave light source) for the modeling of multiple scattering in a laser beam. The off-axis shape coefficients of an arbitrary beam are computed starting from the set of known beam-shape coefficients for an on-axis location by using the addition theorem for the spherical vector wave-

functions of the first kind. The discussed technique is verified by comparison with a localized approximation for a focused Gaussian beam and with Barton's spheres-arbitrary beam interaction theory. An additional advantage of the proposed technique (self-testing of the computation accuracy by comparison of the off-axis beam-shape coefficients evaluated from two different on-axis origins) is demonstrated.

## 1 Introduction

Modeling of multiple scattering of a plane wave [1–8] and a laser beam [9–12] by homogeneous spheres has been a topic of research interest in a variety of areas of practical applications, including the design of optical sizing systems and signal interpretation in such instruments. In our previous papers [13, 14], the formalism of exact electromagnetic wave multiple scattering theory [3, 4] was used for the first time for signal modeling in photon correlation spectroscopy with a plane-wave light source. To extend this formalism to the more practical case with laser beam illumination, one of the well known techniques may be used for simulation of the beam-shape coefficients, e.g. the generalized Lorenz-Mie theory (GLMT) [15, 16], the angular spectrum of plane waves [12, 17, 18] or the translation addition theorem for the spherical vector wavefunctions (SVWFs) [19].

The main advantage of the addition-theorem technique [19] is its validity for an arbitrary beam with known on-axis beam-shape coefficients, which characterize the laser beam along its propagation axis. The more general, off-axis, coefficients are computed starting from the set of the on-axis coefficients by using the addition theorem for the SVWF of the first kind. Recently, an elegant integral representation of the addition-theorem technique [19] was derived taking into account the Davis on-axis beam-shape coefficients. This integral representation is restricted by the Davis coefficients of the first order only and by the TEM<sub>00</sub> beam. The aim of this paper is to extend the application of the addition-theory technique to the case of multiple scattering of an arbitrary beam (including Davis beam of an arbitrary order) by an ensemble of homogeneous spheres.

The body of this paper is organized as follows. A short summary of the multiple scattering of a plane wave by an ensemble of

spheres is given in Section 2.1 for the so-called single/common-origin approach. Increasing the computation efficiency by the multiple-origins approach is discussed briefly in Section 2.2. Relationships between the expansion coefficients of an arbitrary incident beam and its beam-shape coefficients derived by using an addition theorem for the SVWF are presented in Section 2.3. In Section 3, simulated results are compared with data published for the interaction of a single sphere and two spheres with a Gaussian beam and a plane-wave.

## 2 Multiple Order Scattering by an Ensemble of Moving Spheres

### 2.1 Plane Wave Illumination

We assume that a plane wave with wavenumber  $k$  propagates along the  $Z$  axis and illuminates an ensemble of  $N$  spheres positioned in a non-absorbing medium  $L$ . The wavenumber is defined by

$$k = \frac{2\pi n_L}{\lambda}, \quad (1)$$

where  $n_L$  is the refractive index of the medium and  $\lambda$  is the wavelength in vacuum. As in previous papers [13, 14], the scattered electric field,  $\mathbf{E}_s$ , from the entire ensemble of spheres is taken to be the superposition of scattered fields,  $\mathbf{E}_s^i$ , from each of the spheres in the ensemble, i.e.

$$\mathbf{E}_s = \sum_{i=1}^N \mathbf{E}_s^i, \quad (2)$$

where

$$\mathbf{E}_s^i = E_o^i D(\mathbf{X}^i) \sum_{n=1}^{\infty} \sum_{m=-n}^n [a_{mn1}^i \mathbf{N}_{mn}^{(3)}(k\mathbf{R}_d^i) + a_{mn2}^i \mathbf{M}_{mn}^{(3)}(k\mathbf{R}_d^i)], \quad (3)$$

\*Dr. V. I. Ovod, Particle Sizing and Light Scattering Instrumentation, 6621 Picasso Rd., Ste. 16, Goleta, CA 93117 (USA).  
e-mail: vovod@yahoo.com

$\mathbf{R}_d^i$  is the vector between the origin of the particle  $i$  and a point detector  $d$ ,  $\mathbf{X}^i$  is the position vector of the origin of particle  $i$  in the coordinate system of the particle ensemble (which coincides with the XYZ experimental coordinate system), respectively,  $D(\mathbf{X}^i)$  is the relative sensitivity of detector  $d$ , and  $a_{mnp}$  is the scattered field expansions of order  $n$  and degree  $m$ . The extra index  $p$  denotes the mode, in which  $p = 1$  and  $p = 2$  refer to the TM and the TE modes, respectively, of the scattered field. The incident field strength in the  $z^i$  cross-section is given by

$$E_o^i = E_o \exp(ikL_e) \exp\left(-k^{im} \frac{L_{bi}}{2}\right), \quad (4)$$

where  $E_o$  is the field strength of the incident beam,  $L_e$  is the distance that the beam has traveled to the ensemble origin  $e$ ,  $i = (-1)^{1/2}$  is the unit imaginary number and  $L_{bi}$  is the distance the beam has traveled through the suspension of turbidity  $k^{im}$  (in fact,  $k^{im}$  is the imaginary part of the wavenumber of light in a dispersed system) to the origin of particle  $i$ . As we are working in the framework of elastic light scattering, we omit the time-dependent term  $\exp(-i\omega t)$  from all equations, as is the normal practice. The vector of the scattered field  $\mathbf{E}_s^i$ , the vector spherical harmonics  $\mathbf{M}_{mn}$  and  $\mathbf{N}_{mn}$  and the vector  $\mathbf{R}_d^i$  are given in a spherical coordinate system ( $R^i$ ,  $\theta^i$ , and  $\varphi^i$ ) of the sphere  $i$ . The superscript (3) on the coefficients denotes that the coefficients are based on the spherical Hankel functions.

The scattered field expansions  $a_{mnp}^i$  of the order  $n$  and degree  $m$  employing the single-scattered component ( $u = 1$ ) and the multiple-scattering ( $u = 2$ ) can be expressed by

$$a_{mnp,\varepsilon}^i = \sum_{u=1}^2 a_{mnp,\varepsilon}^{i,u}. \quad (5)$$

The subscript  $\varepsilon$  for  $x$  or  $y$  denotes the scattering coefficients calculated for the parallel (along the  $X$  axis) or perpendicular (along the  $Y$  axis) incident polarization, respectively. The single-scattering and the multiple-scattering components can be written as

$$a_{mnp,\varepsilon}^{i,1} = -\alpha_{np}^i p_{mnp,\varepsilon}^i, \quad (6)$$

$$\begin{aligned} a_{mnp,\varepsilon}^{i,2} = & -\alpha_{np}^i \\ & \times \sum_{\substack{j=i \\ j \neq i}}^N \sum_{l \geq 1}^{N_j^i} \sum_{k=-l}^l [A_{klmn}^{(3)}(kR^{ij}, \Theta^{ij}, \Phi^{ij}) a_{mnp,\varepsilon}^j \\ & + B_{klmn}^{(3)}(kR^{ij}, \Theta^{ij}, \Phi^{ij}) a_{mn(3-p),\varepsilon}^j], \end{aligned} \quad (7)$$

where

$$a_{mnp,\varepsilon}^j = \sum_{u=1}^2 a_{mnp,\varepsilon}^{j,u}, \quad (8)$$

$$a_{mnp,\varepsilon}^{j,1} = -\alpha_{np}^j p_{mnp,\varepsilon}^j, \quad (9)$$

and  $\alpha_{n1}$  and  $\alpha_{n2}$  are the well-known TM and TE Lorenz-Mie coefficients of the isolated sphere. The addition coefficients  $A$  and  $B$  of the third kind depend entirely on the distance  $R^{ij}$  and the direction of translation  $\Theta^{ij}$ ,  $\Phi^{ij}$  of origin  $j$  to  $i$ . The expansion coefficients of the incident plane wave propagating in direction  $z$

are given by [3]

$$\begin{aligned} p_{1n1,x}^i &= \frac{-i^{n+1}}{2} \frac{2n+1}{n(n+1)} \exp(ikz^i), \\ p_{-1n1,x}^i &= \frac{i^{n+1}}{2} (2n+1) \exp(ikz^i), \\ p_{mn1,x}^i &= 0, \quad |m| \neq 1, \end{aligned} \quad (10)$$

$$p_{mn(3-p),\varepsilon}^i = m p_{mnp,\varepsilon}^i, \quad p_{mn p,y}^i = \frac{1}{i} p_{mn(3-p),x}^i \quad (11)$$

As we can see, the scattering Eqs. (5) and (8) are written for all  $N$  particles that participate in the scattering, thus producing a set of coupled ( $p = 1, 2$ ) linear Eqs. (5) for the scattered field expansions. The set of these coupled equations is most commonly solved by the order-of-scattering technique [1, 2] or by iteration methods [3–8].

It must be noted that the scattered field expansions for all  $N$  particles are obtained now in their own coordinate systems. Hence the accompanying vector spherical harmonics have to be translated from the individual particle origins back to the common (ensemble) origin. As a result of this translation, the required number of orders,  $N_o^j$ , in the expansions for the scattered field from sphere  $j$  in Eq. (7) is large, because this number depends not only on the size of the sphere but also on the above mentioned translation distance [4]. This last translation (used in our previous investigation [13] in the so-called single/common-origin approach) causes numerical convergence problems that have been discussed comprehensively elsewhere [8]. These problems are eliminated if one is interested in far-zone scattering only. In this case (so-called multiple-origins approach), the last set of translation coefficients has a straightforward analytical form [8], and the required number of orders  $N_o^j$  in the expansions for the scattered field from the  $j$ th sphere depends on the size parameter of this sphere only as shown in Ref. [20] by

$$N_o^j \approx \rho^j + 4(\rho^j)^{1/3} + 2, \quad (12)$$

where  $\rho^j = ka^j$  is the Mie parameter and  $a^j$  is the radius of the  $j$ th sphere.

## 2.2 Far-zone Assumption

Most optical systems for particle sizing are based on the detection of the light scattered in the far zone, when smallest distance  $R_d^i$  for each sphere is larger than the largest distance between the spheres,  $R^{ij}$ . For the far-zone assumption, the spherical Hankel functions can be replaced by their asymptotes [8], and the orthonormal unit vectors  $\mathbf{r}^i$ ,  $\theta^i$ , and  $\varphi^i$  for the  $i$  sphere coincide with the corresponding orthonormal unit vectors  $\bar{\mathbf{r}}$ ,  $\bar{\theta}$ , and  $\bar{\varphi}$  for the entire ensemble. Taking into account the above-mentioned asymptotes of the spherical Hankel function, we can write the vector spherical functions in the far zone [8] as

$$\begin{aligned} \mathbf{M}_{mn}^{(3)}(k\mathbf{R}_d^i) &= (-i)^{n+1} \frac{\exp(i\mathbf{k}_s^i \mathbf{R}_d^i)}{k R_d^i} \exp\left(-k_m^{im} \frac{L_{id}}{2}\right) \\ &\times [i\tau_{mn2}(\theta^i)\bar{\theta} - \tau_{mn1}(\theta^i)\bar{\varphi}] \exp(im\varphi^i), \end{aligned} \quad (13)$$

$$\begin{aligned} \mathbf{N}_{mn}^{(3)}(k\mathbf{R}_d^i) &= (-i)^n \frac{\exp(i\mathbf{k}_s^i \mathbf{R}_d^i)}{k R_d^i} \exp\left(-k_m^{im} \frac{L_{id}}{2}\right) \\ &\times [\tau_{mn1}(\theta^i)\bar{\theta} + i\tau_{mn2}(\theta^i)\bar{\varphi}] \exp(im\varphi^i), \end{aligned} \quad (14)$$

where

$$\tau_{mn1}(\theta) = \frac{d}{d\theta} P_n^m \cos(\theta), \quad \tau_{mn2}(\theta) = \frac{m}{\sin(\theta)} P_n^m \cos(\theta) \quad (15)$$

are the scattering functions,  $P_n^m$  stands for the associated Legendre function of the first kind [3] and  $L_{id}$  is the distance in the suspension from the origin of the particle  $i$  to point detector  $d$ . The scattered wave vector relative to the origin of the particle  $i$  is defined by

$$\mathbf{k}_s^i = \frac{k\mathbf{R}_d^i}{R_d^i} = k(\sin\theta^i \cos\varphi^i \bar{x} + \sin\theta^i \sin\varphi^i \bar{y} + \cos\theta^i \bar{z}), \quad (16)$$

where  $\bar{x}$ ,  $\bar{y}$ , and  $\bar{z}$  are the unit vectors of the Cartesian coordinate system.

We consider that  $R_d^i \approx R_d$  in the far zone and that the relation between the position vectors of sphere  $i$  and detector  $d$  can be expressed by

$$\mathbf{R}_d^i = \mathbf{R}_d - \mathbf{X}^i \quad (17)$$

where  $\mathbf{R}_d$  is the position vector of the detector in the experimental frame.

By inserting Eq. (17) into Eqs. (13) and (14), and then Eqs. (13) and (14) into Eq. (3), we can rewrite the expression for the  $\mathbf{E}_s^i$  field scattered from sphere  $i$  in a form that is suitable for the analysis of particle motion on the signal [14], i.e.

$$\mathbf{E}_s^i = i\mathcal{T}\mathbf{P}_s^i, \quad (18)$$

where

$$T = E_o D(\mathbf{X}^i) \frac{\exp(i\mathbf{k}_s^i \mathbf{R}_d^i)}{k R_d^i} \exp(i k L_e) \exp\left(-k_m^{im} \frac{L_{bi} + L_{id}}{2}\right) \quad (19)$$

is a coefficient which does not depend strongly on the motion of particle  $i$ . The vector scattering amplitude,  $\mathbf{P}_s^i$ , reflects the main contribution of the particle motion to the signal in the photon cross-correlation. The components of vector  $\mathbf{P}_s^i$  of the scattering amplitudes, polarized in the  $\bar{\theta}$  and  $\bar{\varphi}$  directions [6], are expressed by

$$P_\theta^i = \exp(-i\mathbf{k}_s^i \mathbf{X}^i) [S_2^i(\theta^i, \varphi^i) e_x^i + S_3^i(\theta^i, \varphi^i) e_y^i], \quad (20)$$

$$P_\varphi^i = \exp(-i\mathbf{k}_s^i \mathbf{X}^i) [S_4^i(\theta^i, \varphi^i) e_x^i + S_1^i(\theta^i, \varphi^i) e_y^i], \quad (21)$$

where  $e_x^i$  and  $e_y^i$  are the components of the unit polarization vector of the plane wave that illuminates sphere  $i$ , and

$$S_1^i(\theta^i, \varphi^i) = \sum_{n=1}^{\infty} \sum_{m=-n}^n \sum_{p=1}^2 (-i)^n a_{mnp, \varepsilon=y}^i \tau_{mn(3-p)}(\theta^i) \exp(im\varphi^i), \quad (22)$$

$$S_2^i(\theta^i, \varphi^i) = \sum_{n=1}^{\infty} \sum_{m=-n}^n \sum_{p=1}^2 (-i)^{n+1} a_{mnp, \varepsilon=x}^i \tau_{mnp}(\theta^i) \exp(im\varphi^i), \quad (23)$$

$$S_3^i(\theta^i, \varphi^i) = \sum_{n=1}^{\infty} \sum_{m=-n}^n \sum_{p=1}^2 (-i)^{n+1} a_{mnp, \varepsilon=y}^i \tau_{mnp}(\theta^i) \exp(im\varphi^i), \quad (24)$$

$$S_4^i(\theta^i, \varphi^i) = \sum_{n=1}^{\infty} \sum_{m=-n}^n \sum_{p=1}^2 (-i)^n a_{mnp, \varepsilon=x}^i \tau_{mn(3-p)}(\theta^i) \exp(im\varphi^i), \quad (25)$$

are the four elements of the amplitude scattering matrix [5, 6]. As mentioned above, the subscript  $\varepsilon$  for  $x$  or  $y$  denotes a scattering coefficient calculated for parallel (along the  $X$  axis) or perpen-

dicular (along the  $Y$  axis) incident polarization, respectively. We assume the same polarization of the incident wave for all particles, i.e.

$$e_x^i = \frac{E_x}{E_o}, \quad (26)$$

$$e_y^i = \frac{E_y}{E_o}, \quad (27)$$

where  $E_x$  and  $E_y$  correspond to incident plane wave polarization in the  $\bar{x}$  and  $\bar{y}$  directions, respectively, in the cross-section of the light emission.

The exponential coefficient in Eqs. (20) and (21) is the product of Eq. (17) in the above-mentioned multiple-origins scattering approach, and its use eliminates the last translation of the partial wave scattering amplitudes  $a_{mnp, \varepsilon}^i$  in Eqs. (22)–(25) from the origin of each sphere to the common (ensemble) origin. This exponential coefficient confirms that our model is in agreement with published results [8] based on deriving the analytical expression for the vector coefficients of the last translations to the common origin. The computation efficiency of the multiple-origins approximation of the scattering by a particle ensemble in the far zone was investigated recently [8] in comparison with the single-origin approximation for the far-field scattering [3].

### 2.3 Arbitrary Beam Illumination

The core of the proposed upgrade strategy is the off-axis expansion coefficients  $p_{mnp, \varepsilon}^i$  of an arbitrary beam at the origin of the  $i$ th sphere. If an on-axis origin,  $e$ , is chosen on the  $Z$  axis of the laser beam, these coefficients can be simulated by using a translation addition theorem for spherical vector wave functions [19], i.e.

$$p_{mnp, \varepsilon}^i = \sum_{l \geq 1} \sum_{k=-l, k \neq 0}^l (A_{klmn}^{(1)}(k R^{ie}, \Theta^{ie}, \Phi^{ie}) P_{klp, \varepsilon}^e + B_{klmn}^{(1)}(k R^{ie}, \Theta^{ie}, \Phi^{ie}) P_{kl(3-p), \varepsilon}^e). \quad (28)$$

The addition coefficients  $A$  and  $B$  of the first kind depend on the distance  $R^{ie}$  and the direction of translation  $\Theta^{ie}$ ,  $\Phi^{ie}$  of the on-axis origin  $e$  to the origin of the  $i$ th sphere. The expansion coefficients at the on-axis origin can be expressed by

$$p_{m=\pm 1n p=1, x}^e = P_{m=\pm 1n p=1, x}^{plane} g_n^e, \quad (29)$$

where the on-axis coefficients  $g_n^e$  are defined in the classical beam-shape formalism [15], and

$$p_{m=\pm 1n 1, x}^{plane} = \frac{1}{2} C_{m=\pm 1n} \quad (30)$$

are the well know expansion coefficients for the plane-wave incident field [5]. The normalized constant  $C_{mn}$  can be expressed as in Ref. [19]:

$$C_{mn} \begin{cases} C_n & m \geq 0 \\ (-1)^{|m|} \frac{(l+|m|)!}{(l-|m|)!} C_n & m < 0 \end{cases} \quad (31)$$

where

$$C_n = i^{n-1} \frac{(2n+1)}{n(n+1)}. \quad (32)$$

It is evident that coefficients defined by Eqs. (10) and (30) coincide where  $z^i = 0$ . To evaluate the TE and y-polarized on-axis

expansion coefficients  $p_{\pm 1np,e}^e$ , one can use Eq. (11), which was defined for the plane-wave expansion coefficients.

According to the presented formalism, the classical on-axis coefficients  $g_n^e$  are taken as starting coefficients for an arbitrary incident beam. To simulate the starting on-axis coefficients for a Gaussian laser beam, any known analytical expression for  $g_n^e$  can be used [21]. In our simulations we use the modified localized approximation [15] for the high-order Davis beam, i.e.

$$g_n^e = Q \exp[-(n-1)(n+2)Qs^2] \exp(ikz^e) \quad (33)$$

and the  $\mu$ th-order Barton symmetrized beam [15, 21], which is given by

$$g_n^{e,\mu} = \sum_{j=0}^{j+2l=2\mu+1} \sum_{l=0} \left( \frac{-2isz^e}{\omega_o} \right) (-1)^l s^{2l} \times \frac{(l+j)!}{l!j!} \frac{1}{l!} \frac{(n-1)!}{(n-1-l)!} \frac{(n+1+l)!}{(n+1)!} \exp(ikz^e), \quad (34)$$

where the on-axis origin  $e$  is characterized by the  $z^e$  coordinate. The fundamental parameter related to the waist radius  $\omega_o$  is defined by

$$s = \frac{1}{k\omega_o} \quad (35)$$

and

$$Q = \frac{1}{1 + 2isz^e/\omega_o}. \quad (36)$$

If one is interested in the Davis beam of the first order only, characterized by the first-order on-axis coefficients, which are defined by

$$g_n^e = Q \exp[-(n+0.5)^2 Qs^2] \exp(ikz^e), \quad (37)$$

the integral representation technique [19] can be used as an effective solution of Eq. (28).

Relationships between two kinds of off-axis beam-shape coefficients (defined in the classical formalism and in the presented technique) can be expressed at the origin of sphere  $i$  by

$$g_{mnTM,\varepsilon}^i = \frac{1}{C_{mn}} P_{mp=1,\varepsilon}^i \quad (38)$$

and

$$(ig_{mnTE,\varepsilon}^i) = \frac{1}{C_{mn}} P_{mp=2,\varepsilon}^i. \quad (39)$$

### 3 Numerical Results

The formulation presented in this paper has been used to upgrade the computer code developed recently for the signal modeling in photon correlation/cross-correlation spectroscopy [13, 14]. The code involves numerical algorithms developed by *Mackowski* [3, 4] for the addition coefficients  $A$  and  $B$ , and for solving of coupled ( $p = 1, 2$ ) linear Eqs. (5) for the scattered field expansions when the single/common origin approach is used. We do not intend to discuss the numerical results in detail. Numerical calculations are presented to illustrate the correctness of the upgraded code by comparison with published data.

Table 1 shows a quantitative comparison of the localized approximation method (data are borrowed from Ref. [19] for an  $x$ -polarized Gaussian TEM<sub>00</sub> beam with  $\omega_o = 5 \mu\text{m}$ ,  $\lambda = 0.5 \mu\text{m}$ ,  $n_L = 1$ ,  $x^i = y^i = 2 \mu\text{m}$ ,  $z^i = 10 \mu\text{m}$ ) and the addition-theorem method concerning the values of the  $g_{mn,TM}^i$ . The analytical

Table 1: Comparison of  $g_{mn,TM}^i$  off-axis coefficients computed by localized approximation and addition theorem:  $x^i = y^i = 2 \mu\text{m}$ ,  $z^i = 10 \mu\text{m}$ ,  $\lambda = 0.5 \mu\text{m}$ ,  $\omega_o = 5 \mu\text{m}$ .

5(m+n)	Re ( $g_{mn,TM}$ )		Im ( $g_{mn,TM}$ )	
	Localized approximation	Addition theorem	Localized approximation	Addition theorem
1	9.82716E-04	-9.83516E-04	9.16325E-03	-9.16683E-03
2	2.94447E-03	-2.94684E-03	2.74665E-02	-2.74776E-02
3	5.87785E-03	-5.88258E-03	5.48635E-02	-5.48853E-02
4	9.77181E-03	-9.77968E-03	9.12850E-02	-9.13239E-02
5	1.46116E-02	-1.46234E-02	1.36638E-01	-1.36696E-01
6	3.62323E-01	3.62568E-01	-1.57210E-02	-1.57457E-02
7	3.62064E-01	3.62308E-01	-1.57598E-02	-1.57840E-02
8	3.61676E-01	3.61920E-01	-1.58172E-02	-1.58412E-02
9	3.61159E-01	3.61402E-01	-1.58935E-02	-1.59174E-02
10	3.60514E-01	3.60755E-01	-1.59882E-02	-1.60110E-02
12	-2.53439E-03	2.53663E-03	-2.04327E-03	2.04479E-03
13	-2.53117E-03	2.53339E-03	-2.04061E-03	2.04215E-03
14	-2.52688E-03	2.52918E-03	-2.03707E-03	2.03861E-03
15	-2.52153E-03	2.52381E-03	-2.03266E-03	2.03425E-03

expression Eq. (34) for the fifth-order Barton symmetrized beam [15] is used to simulate the starting on-axis coefficients  $g_n^e$  at  $z^e = z^i = 10 \mu\text{m}$ . The cumulative relative differences for the real and imaginary parts, which are less than 0.12%, confirms the good agreement between the two techniques. Different signs are caused by the fact that the definition of the Legendre functions  $P_n^m$  in the two compared techniques differs by the coefficient  $(-1)^m$  [3, 19].

It must be noted that the additional advantage of the described technique is that it permits the self-testing of the computation accuracy by comparison of the off-axis beam coefficients evaluated from two different on-axis origins, for example, from  $z^e = 0$  and from  $z^e = z^i$  (where  $z^i$  is the coordinate of the  $i$ th sphere along the  $Z$  axis). The cumulative relative difference, CRD, for the real and imaginary parts defined by

$$CRD = \frac{1}{2} \left[ \left| \frac{\text{Re}(g_{mn,TM,\varepsilon}^i(z^i)) - \text{Re}(g_{mn,TM,\varepsilon}^i(0))}{\text{Re}(g_{mn,TM,\varepsilon}^i(z^i))} \right| + \left| \frac{\text{Im}(g_{mn,TM,\varepsilon}^i(z^i)) - \text{Im}(g_{mn,TM,\varepsilon}^i(0))}{\text{Im}(g_{mn,TM,\varepsilon}^i(z^i))} \right| \right] \quad (40)$$

is shown in Figure 1 for the  $x$ -polarization of the fifth-order Barton symmetrized beam with  $\omega_o = 5 \mu\text{m}$ ,  $\lambda = 0.5 \mu\text{m}$ ,  $n_L = 1$ ,  $x^i = y^i = 2 \mu\text{m}$  and  $z^i = 10 \mu\text{m}$ . The fact that the CDR is less than 0.031% confirms the high accuracy of the addition-theorem technique and the effectiveness of the self-testing that is available with it.

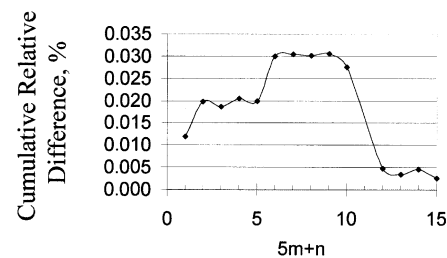


Fig. 1: Cumulative relative differences for the real and imaginary parts of  $g_{mn,TM,x}^i$  computed in addition-theorem technique from two different on-axis origins ( $z^e = 0$  and  $z^e = z^i$ ) for the fifth-order Barton symmetrized beam with  $\omega_o = 5 \mu\text{m}$ ,  $\lambda = 0.5 \mu\text{m}$ ,  $n_L = 1$ ,  $x^i = y^i = 2 \mu\text{m}$ ,  $z^i = 10 \mu\text{m}$ .

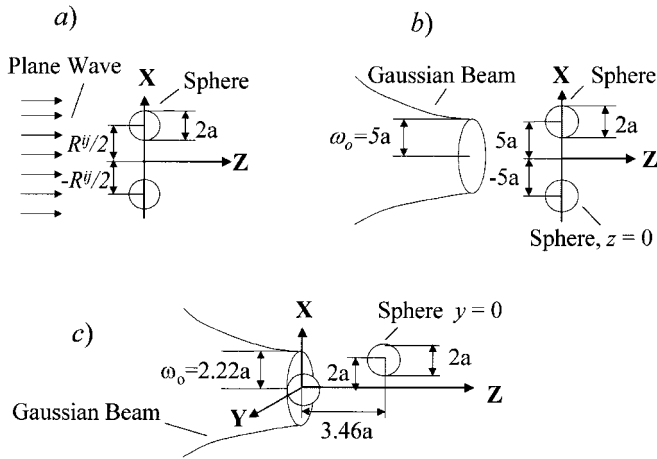


Fig. 2: Scattering schemes modeled in this paper to illustrate the correctness of the upgraded code by comparison with data published in Refs. [8] and [9]. Two spheres are illuminated by a plane wave (a) or a Gaussian beam of the waist radius  $\omega_o = 5a$  and  $\omega_o = 2.22a$  (b and c, respectively). Each sphere of radius  $a = \rho/k$  has a size parameter of  $\rho = 3.083$  (a and b) and  $\rho = 11$  (c). The refractive index of each sphere is  $1.61 + i0.004$  (a and b) and  $1.334 + i1.2 \times 10^{-9}$  (c) in a medium of refractive index  $n_L = 1$ . In (c), two spheres are positioned in a Gaussian beam at  $(x = y = z = 0)$  and  $(x = 2a, y = 0, z = 3.46a)$ , respectively.

Figure 2 illustrates three schemes for the interaction of two spheres with a plane wave (Figure 2a) and with a Gaussian beam of the waist radius  $\omega_o = 5a$  and  $\omega_o = 2.22a$  (Figure 2b and c, respectively). Each sphere of radius  $a = \rho/k$  has a size parameter  $\rho = 3.083$  (Figure 2a and b) and  $\rho = 11$  (Figure 2c). The refractive index of each sphere is  $1.61 + i0.004$  (Figure 2a and b) and  $1.334 + i1.2 \times 10^{-9}$  (Figure 2c) in a medium of refractive index  $n_L = 1$ . In Figure 2c, two spheres are positioned in a Gaussian beam at  $(x = y = z = 0)$  and  $(x = 2a, y = 0, z = 3.46a)$ . The multiple scattering effects are modeled for these three schemes to compare with results published in Refs. [8] and [9]. Figures 3 and 4 refer to the illumination of two spheres by a plane wave as shown in Figure 2a and in Ref. [8]. The center-to-center separation is chosen as  $R^{ij} = 2.6a$  (Figure 3) and  $R^{ij} = 10a$  (Figure 4). Angular distributions of the scattering intensity  $i_{22}$  in Figure 3 and intensity  $i_{11}$  in Figure 4 are given on a semi-logarithmic scale for the single-origin approach (SO) and the multiple-origins approach (MO). The scattering intensities are defined by

$$i_{11} = |S_1(\theta, 0)|^2, \quad i_{22} = |S_2(\theta, 0)|^2. \quad (41)$$

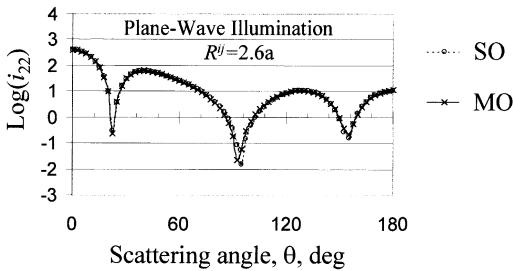


Fig. 3: Angular distributions of the scattering intensity  $i_{22}$  from two spheres of radius  $a$  illuminated by a plane wave (see Figure 2a, center-to-center separation  $R^{ij} = 2.6a$ ). Comparison between the single-origin approach (SO) and the multiple-origins approach (MO). The required number of scattering terms,  $N_O$ , for the SO approach and the MO approach is 15 and 9, respectively.

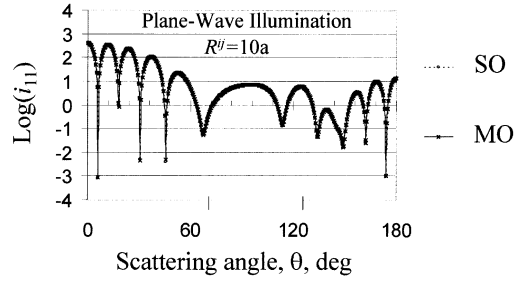


Fig. 4: Angular distributions of the scattering intensity  $i_{11}$  from two spheres of radius  $a$  illuminated by a plane wave (see Figure 2a, intersphere separation  $R^{ij} = 10a$ ): Comparison between the single-origin approach (SO) and the multiple-origins approach (MO). The required number of scattering terms,  $N_O$ , for the SO approach and the MO approach is 26 and 9, respectively.

The required number of scattering terms,  $N_O$ , for the single-origin approach is 15 if  $R^{ij} = 2.6a$  and 26 if  $R^{ij} = 10a$ . Figures 3 and 4 show a negligible difference between the SO approach and the more efficient MO approach which requires only  $N_O = 9$  scattering terms. The angular distribution of  $i_{22}$  for an intersphere separation  $R^{ij} = 2.6a$  in Figure 3 and  $i_{11}$  for  $R^{ij} = 10a$  in Figure 4 are in good agreement with results published recently [8] (Figures 1, 3 and 6).

As mentioned above, the discussed technique permits modeling of the multiple-scattering effects in an arbitrary beam. Figures 5 and 6 illustrate a multiple scattering simulation in Gaussian beams. Figure 5 shows the angular distribution of the scattering intensity  $i_{11}$  from two spheres of radius  $a$  positioned with intersphere separation of  $R^{ij} = 10a$  in the Gaussian beam as shown in Figure 2b.

As an additional verification of the proposed technique, Figure 6 illustrates the normalized intensity (the time-averaged Poynting

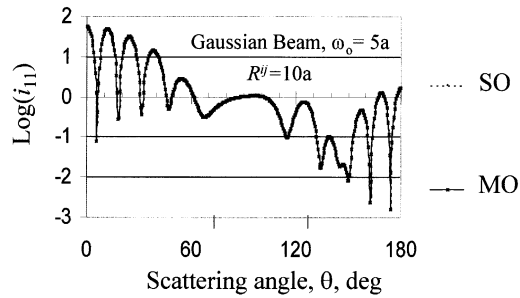


Fig. 5: Angular distribution of the scattering intensity  $i_{11}$  from two spheres of radius  $a$  with intersphere separation  $R_{ij} = 10a$  positioned in a Gaussian beam as shown in Figure 2b.

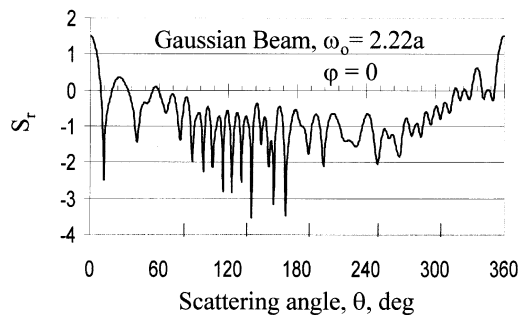


Fig. 6: Normalized scattering intensity  $S_t$  as a function of angle in the  $x - z$  plane for two spheres positioned as shown in Figure 2c.

vector) in one of Barton's known scattering schemes (see Figure 2c). This scheme [9] is characterized by two spheres of size parameter  $\rho = 11$  (radius  $a = \rho/k$ ) and refractive index  $1.334 + i1.2 \times 10^{-9}$ , that positioned at  $(x = y = z = 0)$  and  $(x = 2a, y = 0, z = 3.46a)$ , respectively, in a Gaussian beam of waist radius  $\omega_o = 2.22a$  as shown in Figure 2c. The time-averaged Poynting vector is defined by

$$S_r = \frac{|S_2(\theta, \varphi = 0)|^2 + |S_4(\theta, \varphi = 0)|^2}{\pi\rho^2}. \quad (42)$$

The angular distribution of the normalized intensity  $S_r$  presented in Figure 6 is in good agreement with published data Ref. [9] (Figure 7).

## 4 Conclusions

Direct use of the addition theorem for the spherical vector wave function has been demonstrated for the evaluation of the beam-shape coefficients in the general case of an off-axis location of the scatterer. In contrast with the integral representation of the translation coefficients [19], this technique is valid for an arbitrary beam with known on-axis expansion coefficients. The discussed technique is verified by comparison with localized approximation of a focused Gaussian beam, and it was integrated in the code [13, 14] for modeling of multiple scattering effects. Results obtained by this upgraded code are in good agreement with published data [8, 9]. An additional advantage of the proposed technique (self-testing of the computation accuracy by comparison of the off-axis beam-shape coefficients evaluated from two different on-axis origins) is demonstrated. The most effective application of the addition-theorem technique is the signal simulation in dynamic light scattering [13, 14]. This technique can also be used in signal modeling for particle counters/sizers [6] and phase-Doppler anemometry [11].

## 5 Symbols and Abbreviations

$A, B$	addition coefficients
$a^j$	radius of sphere $j$
$a_{mnp}$	scattered field expansions
$C_{mn}$	normalized constant
CRD	cumulative relative differences
$D$	relative sensitivity of detector
$d$	subscript for the point detector
$d_p^j$	diameter of the $j$ th sphere
$\mathbf{E}_s$	scattered electric field
$E_o$	field strength of the incident beam
$e_x, e_y$	components of the polarization vector of the incident field
$g_{mn}$	classical beam-shape coefficients
$i$	unit imaginary number
$i, j$	superscripts for sphere $i$ and sphere $j$ , respectively
$i_{11}, i_{22}$	scattering intensities
$k$	wavenumber
$k^{im}$	imaginary part of the wavenumber of light in a dispersed system (turbidity)
$L_{bi}$	distance the beam has traveled through the suspension to the origin of particle $i$
$L_e$	distance that the beam has traveled to the ensemble origin $e$

$L_{id}$	distance in the suspension from the origin of particle $i$ to point detector $d$
$\mathbf{M}_{mn}, \mathbf{N}_{mn}$	vector spherical harmonics
MO	multiple-origin approach
$m$	subscript that denotes the degree of the field expansions
$N$	total number of spheres in the cell
$N_o^j$	required number of orders in the expansions for the scattered field from sphere $j$
$n$	subscript that denotes the order of the field expansions
$n_L$	refractive index of a non-absorbing medium
$P_n^m$	associated Legendre function
$\mathbf{P}_s^i$	vector scattering amplitude for sphere $i$
$P$	subscript that refers to the TM ( $p = 1$ ) or the TE ( $p = 2$ ) mode
$P_{mnp,e}^i$	coefficients of an arbitrary beam at the origin of the $i$ th sphere
$Q$	parameter in localized approximation for a focused Gaussian beam
$(R, \theta, \varphi)$	spherical coordinate system
$R^{ij}$	intersphere separation
$\mathbf{R}_d$	position vector of the point detector relative the origin of the particle ensemble
$S_1 - S_4$	elements of the amplitude scattering matrix
SO	single-origin approach
$S_r$	normalized intensity (the time-averaged Poynting vector)
$s$	fundamental parameter in localized approximation for a focused Gaussian beam
$T$	coefficient which does not depend strongly on the motion of a particle
TE	transverse electric
TM	transverse magnetic
$\mathbf{X}$	position vector
$\bar{x}, \bar{y}, \bar{z}$	unit vectors of the Cartesian coordinate system
$u$	superscript that denotes order of scattering ( $u = 1$ corresponds to single scattering, $u = 2$ corresponds to multiple scattering)
$\alpha_{n1}, \alpha_{n2}$	TM and TE Lorenz-Mie coefficients of an isolated sphere, respectively
$\varepsilon$	subscript that denotes $X(\varepsilon = x)$ or $Y(\varepsilon = y)$ polarization of the incident beam
$\lambda$	wavelength
$\rho$	Mie parameter
$\tau_{mnp}$	scattering functions
$\omega_o$	waist radius of the incident beam

## 6 References

- [1] K. A. Fuller, G. W. Kattawar: Consummate solution to the problem of classical electromagnetic scattering by an ensemble of spheres. 1: Linear chains. Opt. Lett. 13 (1988) 90–92.
- [2] K. A. Fuller, G. W. Kattawar: Consummate solution to the problem of classical electromagnetic scattering by an ensemble of spheres. 2: Clusters of arbitrary configuration. Opt. Lett. 13 (1988) 1063–1065.
- [3] D. W. Mackowski: Analysis of radiative scattering for multiple sphere configuration. Proc. R. Soc. London A 433 (1991) 599–614.
- [4] D. W. Mackowski: Calculation of total cross sections of multiple-sphere clusters. J. Opt. Soc. Am. A 11 (1994) 2851–2861.
- [5] D. W. Mackowski, M. I. Mischenko: Calculation of the T matrix and scattering matrix for ensembles of spheres. J. Opt. Soc. Am. A 13 (1996) 2266–2278.

- [6] *G. Videen, R. G. Pinnick, D. Ngo, Q. Fu, P. Chylek*: Asymmetric parameter and aggregate particles. *Appl. Opt.* 37 (1998) 1104–1109.
- [7] *Y.-L. Xu*: Electromagnetic scattering by an aggregate of spheres. *Appl. Opt.* 34 (1995) 4573–4588.
- [8] *Y.-L. Xu*: Electromagnetic scattering by an aggregate of spheres: far field. *Appl. Opt.* 36 (1997) 9496–9508.
- [9] *J. P. Barton, W. Ma, S. A. Schaub, D. R. Alexander*: Electromagnetic field for a beam incident on two adjacent spherical particles. *Appl. Opt.* 34 (1991) 4706–4715.
- [10] *J. P. Barton*: Electromagnetic field calculations for a sphere illuminated by a higher-order Gaussian beam. II. Far-field scattering. *Appl. Opt.* 37 (1998) 3339–3344.
- [11] *H. Dahl, T. Wriedt*: The simulation of phase-Doppler anemometry by the multiple multipole method. *Part. Part. Syst. Charact.* 14 (1997) 181–185.
- [12] *H. Bech, A. Leder*: Numerical investigations concerning two-particle scattering in the field of a laser beam on the base of the Fourier-Lorenz-Mie theory. *Proc. Third Workshop on Electromagnetic and Light Scattering – Theory and Applications, T. Wriedt, Y. Eremin* (eds.), University of Bremen, Germany, 1998, pp. 29–36.
- [13] *V. I. Ovod, D. W. Mackowski, R. Finsy*: Modeling of the effect of multiple scattering in photon correlation spectroscopy: plane-wave approach. *Langmuir* 14 (1998) 2610–2618.
- [14] *V. I. Ovod*: Modeling of multiple scattering suppression by a one-beam cross-correlation system. *Appl. Opt.* 37 (1998) 7856–7864.
- [15] *G. Gouesbet, J. A. Lock, G. Gréhan*: Partial-wave representation of laser beams for use in light-scattering calculations. *Appl. Opt.* 34 (1995) 2133–2143.
- [16] *K. F. Ren, G. Gouesbet, G. Gréhan*: Integral localized approximation in generalized Lorenz-Mie theory. *Appl. Opt.* 37 (1998) 4218–4225.
- [17] *A. Doicu, T. Wriedt*: Plane wave spectrum of electromagnetic beams. *Opt. Commun.* 136 (1996) 114–124.
- [18] *E. E. Khaled, S. C. Hill, P. W. Barber*: Scattered an internal intensity of a sphere illuminated with a Gaussian beam. *IEEE Trans. Antennas Propag.* 41 (1993) 295–303.
- [19] *A. Doicu, T. Wriedt*: Computation of the beam-shape coefficients in the generalized Lorenz-Mie theory by using the translation addition theorem for spherical vector wave functions. *Appl. Opt.* 36 (1997) 2971–2978.
- [20] *W. J. Wiscombe*: Improved Mie scattering algorithms. *Appl. Opt.* 19 (1980) 1505–1509.
- [21] *J. A. Lock, G. Gouesbet*: Rigorous justification of the localized approximation to the beam-shape coefficients in generalized Lorenz-Mie theory. I. On-axis beams. *J. Opt. Soc. Am. A* 11 (1994) 2503–2515.